Essential Readings in Light Metals: Aluminum Reduction Technology.
Edited by Geoff Bearne, Marc Dupuis and Gary Tarcy.

 From ***Light Metals 2007***, Morton Sørlie, Editor

BUBBLE NOISE FROM SØDERBERG POTS

Marianne Jensen, Tor Bjarne Pedersen, Kjell Kalgraf
Elkem Aluminium ANS Research, Kristiansand, Norway

Keywords: Aluminium, Søderberg, Bubble noise, Anode

Abstract

High frequency measurements of voltage were introduced at Elkem Aluminium Lista in order to find the effect of noise from the release of gas bubbles under the anode – bubble noise. On a Søderberg pot the bubble noise represents a fairly large portion of the total pot noise. Hence it is important to understand what impacts the bubble noise in order to understand and control the Søderberg pot in a better way.
The bubble noise varies quite a lot over time and between pots. The variations are related to different process conditions. Looking at number of anode problems and carbon dust generation there is a correlation between the bubble noise and the quality of the Søderberg anode. The metal quality is also strongly impacted by a change in the bubble noise. Several process conditions have been investigated, presented and discussed in the paper.

Introduction

Elkem Aluminium Lista (EAL) is a smelter owned by Elkem Aluminium. EAL started to measure bubble noise on all pots in the beginning of 2004. All pots have the New Søderberg Point Feeder Technology developed by Elkem Aluminium (1,2).

The bubble noise is determined as 2.5 minutes averages of 3 seconds peak to peak values of pot voltage. The sampling interval is 0.2 seconds.

Bubble noise by time

In the beginning of 2004 the bubble noise level was approximately 130 mV (fig1). The same year the bubble noise level decreased to approximately 70mV and has stayed at that level since early 2005.

The development has been parallel in all potrooms. This indicates that the big changes in bubble noise are related to some common factor for all the potrooms.

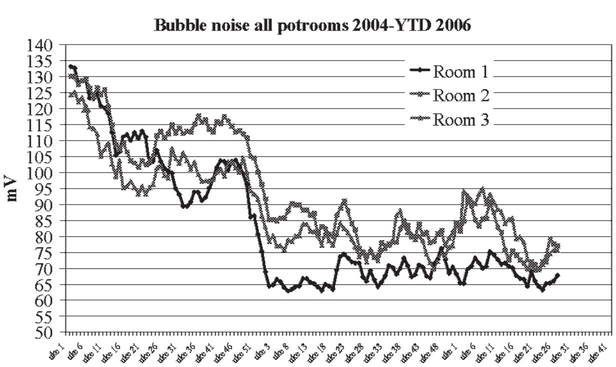

Figure 1. Average values of bubble noise since the beginning of 2004 at EAL.

The bubble noise level in individual pots can have very different levels and also have a different progress over time (fig 2). This fact must be related to individual factors.

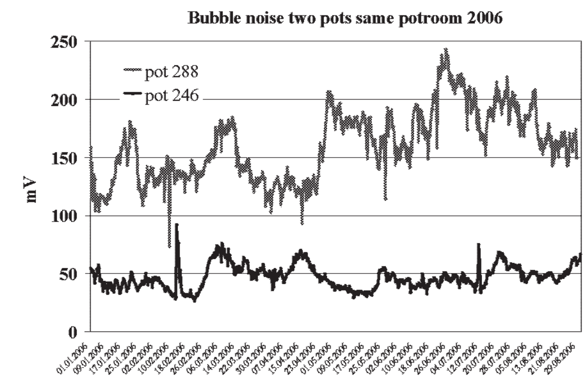

Figure 2. Bubble noise from two individual pots from the same potroom in the same time period.

Bubble noise and anode problems

An anode problem is defined as a piece of carbon coming from the anode that needs to be removed from the pot or anode. The problem can come from an anode deformation, a leak or from pieces falling off the anode. The anode problems are logged for statistical analysis related to the pot operation.

Figure 3 shows the development of the bubble noise and number of anode problems for all potrooms since the beginning of 2004. Figure 4 shows the correlation between these two parameters.

The correlation is good, with a negative correlation coefficient of 0.7. Thus higher bubble noise correlates with fewer anode problems and hence a better anode quality.

Bubble noise can be a tool in the follow-up of the anode quality.

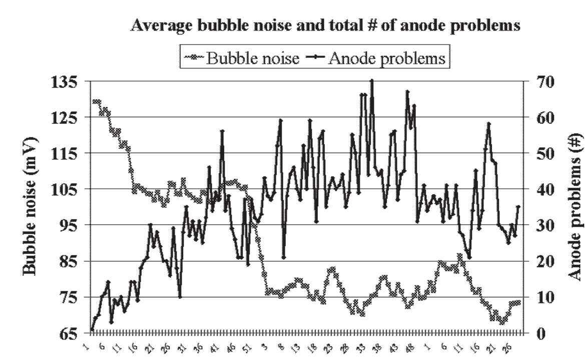

Figure 3. Average bubble noise and total number of anode problems all potrooms.

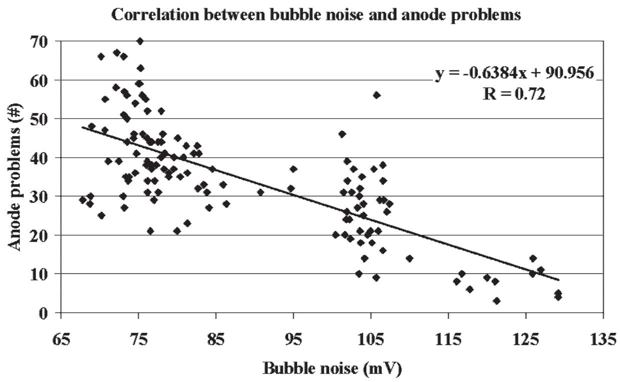

Figure 4. Relationship between bubble noise and anode problems.

Bubble noise and carbon dust

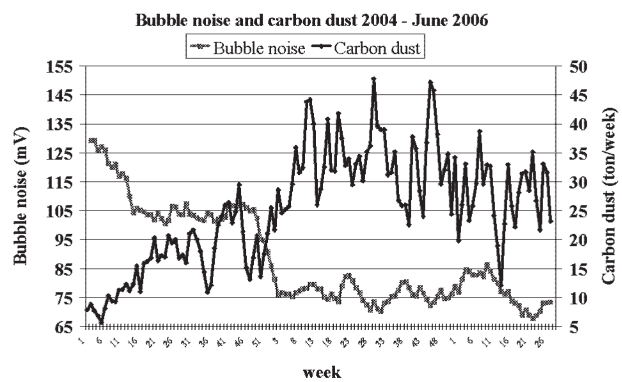

Figure 5. Average bubble noise and carbon dust since the beginning of 2004.

As for number of anode problems, figure 5 also shows a good relationship between bubble noise and amount of carbon dust. The carbon dust includes all material skimmed from the pot. The carbon content i approximately 30% of this material.

The correlation coefficient as shown in figure 6, is even better than for anode problems. It is close to 0.8.

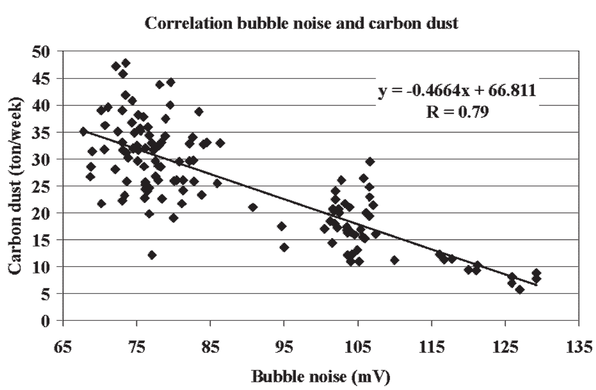

Figure 6. Correlation between bubble noise and carbon dust.

Carbon dust is related to the anode quality. A pot with high levels of carbon dust will also have bigger and more cracks in the anode. This correlation led us to believe that bubble noise may be connected to the cracks in the anode, i.e. anode quality. Hence, higher bubble noise should indicate fewer and smaller cracks and therefore less carbon dust.

Bubble noise and spike setting

All stubbing operators are assigned to their own group of pots. Hence various anode performance data can be monitored for each operator, included bubble noise. The bubble noise level is different for the different stubbing operators, but most of the spike setters have the same development (common pattern) in the bubble noise over time.

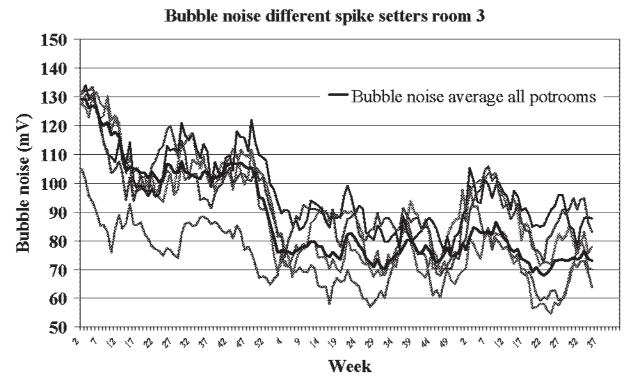

Figure 7. Bubble noise since early 2004 for different stubbing operators in the same potroom.

Figure 7 shows that different spike pullers from one potroom that have different level of bubble noise on their pots. However, the development of bubble noise over time is similar for all the spike pulling operators. The difference in level can be a result of different ways of doing the stubbing operation or different skills.

Some stubbing operators do not always have the same development of the bubble noise over time as shown in figure 8.

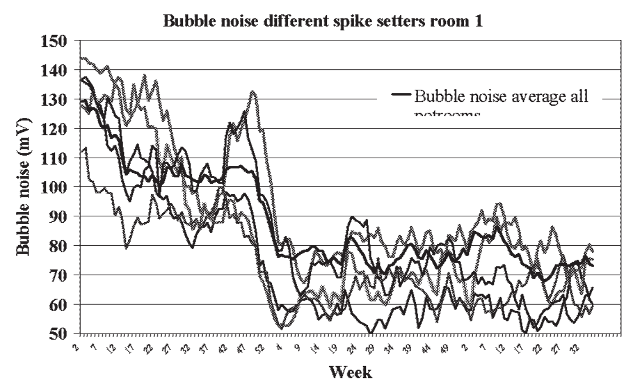

Figure 8. Bubble noise for different stubbing operators, here in potroom number 1, do not always follow the common pattern.

This difference in development can not be explained by any common factor as variation in the anode paste quality. It must be connected to the particular group of pots and most likely to the stubbing operation. The stubbing operation may overshadow effects of common factors. Pots with low bubble noise levels are less likely to follow the common patterns of other groups of pots. Bubble noise can be a good tool in the follow-up of the stubbing operation.

Bubble noise and anode paste

Bubble noise has been compared to many different process variables in the paste plant. So far no correlation has been found between any of the parameters from the paste production and bubble noise. However, this does not exclude other such correlations. Some of the parameters that have been investigated:

- CO_2 reactivity
- Green density
- Blaine figures for ball mill dust
- Coke and pitch temperature
- Amount of particles above 0.075 mm in the dry aggregate mix
- Visual judgment anode top condition

Bubble noise and iron content in metal

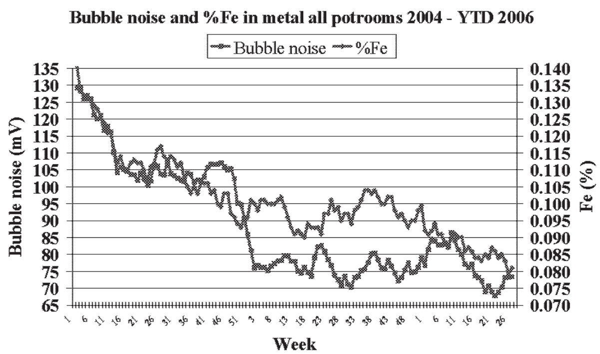

Figure 9. Bubble noise and iron content in metal.

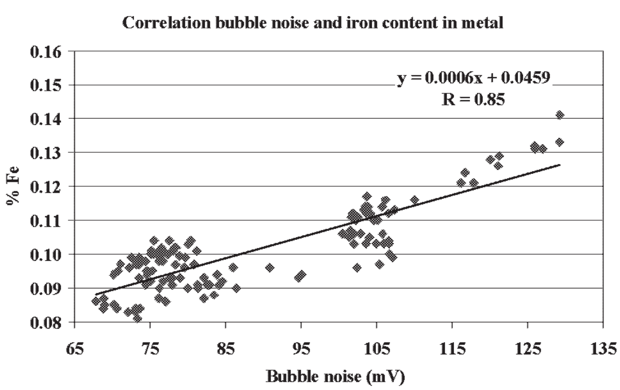

Figure 10. The figure shows the correlation between the bubble noise and iron in metal.

Iron contamination in the metal may vary by a factor of two when bubble noise varies, as shown in figures 9 and 10. Higher bubble noise correlates to a higher iron concentration. Data shows that the increase of iron content comes from the pot gas manifolds and that more iron is eroded when bubble noise is high than when it is low.
This correlation may be connected to the observation that is done for bubble noise and carbon dust. Fewer and smaller cracks are correlated to less carbon dust a higher bubble noise. Higher bubble noise also correlates to higher gas manifold erosion. Hence it is anticipated that the higher rate of erosion is connected to more bath splashing on the gas manifolds since less of the gas will be released through cracks in the anode.
Another theory is also that more carbon dust in the pots will act as damper for bath splashing against the gas manifolds.

Bubble noise and bath height

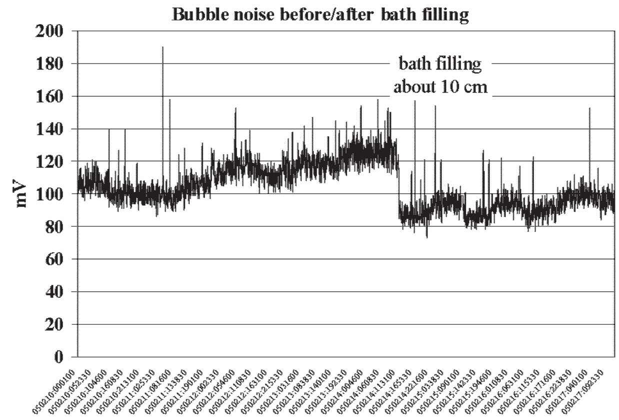

Figure 11. Change of bubble noise in a single pot when adding 10 cm of bath

In a single pot, bubble noise was reduced by 30 mV when 10 cm of bath was added, as shown in Figure 11. The bubble noise was measured every 2.5 minutes. This gives a reduction of 3 mV/cm of bath added. The effect is seen immediately and the bubble noise stays at the lower level. There is little doubt about the cause of this change.

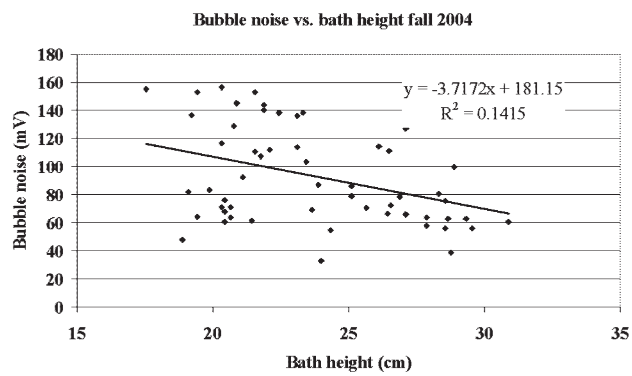

Figure 12. Statistical relationship between bubble noise and bath height for pots in normal operation.

Statistical analysis of many pots in normal operation gives similar effects as shown in Figure 8, where the decline is 3.7 mV/cm of bath added. There is a considerable spread in the values because the anode quality varies a lot between pots. The trend value estimated is of the same magnitude as that measured in a single pot

A study of pots with high and low bath level over time also show that bubble noise is higher for pots with low bath level.

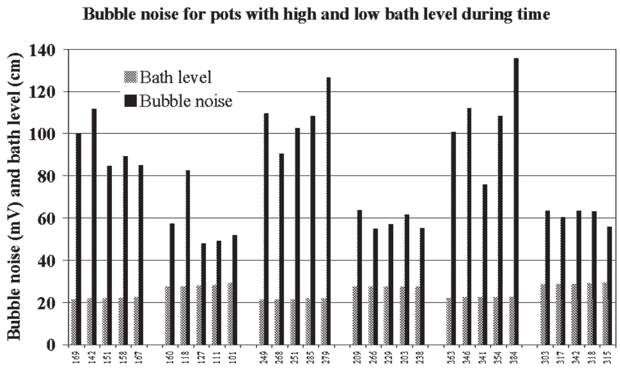

Figure 13. Bubble noise for pots with low and high bath level over time. The bath level is shown on the same axis as the bubble noise.

The change in bubble noise is 7.0 mV/cm between pots with high and low bath level over time. This is about twice as high as measured with an immediate change in bath level. This indicates that a change in bath level has a long term effect in addition to the short term effect.
The long term effect may be that a high bath level over time gives bigger and or more cracks in the anode, and higher gas released through the anode, and therefore a lower bubble noise.

Bubble noise and pot resistance

Increasing the pot resistance is a commonly used action in order to reduce pot noise. This will dampen a metal wave noise, but will not affect the bubble noise. In this case an increase in the resistance will increase the bath temperature and disturb the heat balance in the pot.

Bubble noise and bath acidity

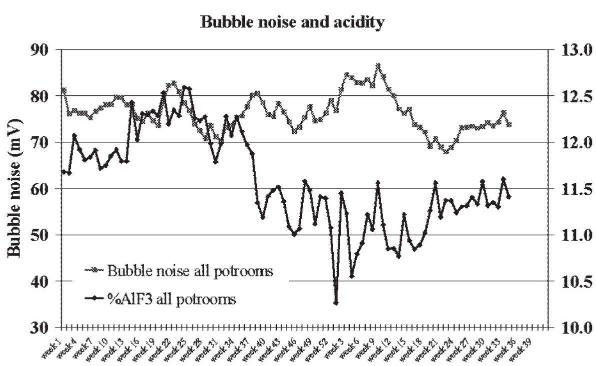

Figure 14. Bubble noise and bath acidity, as average for all potrooms.

There has not been found any correlation between bath acidity and bubble noise.

Conclusion

- There is a relationship between anode quality and bubble noise. Higher bubble noise means better anode quality.
- Bubble noise can be used to detect differences in the spike setting procedure.
- Higher bubble noise correlates to more splashing and higher erosion of gas manifolds.
- Higher bath level gives lower bubble noise.
- High bath level over time gives even lower bubble noise, i.e. more cracks in the anode.

References

1) T.B.Pedersen et al., “Results from implementation of point feeders and complete hooding on VS Søderberg pots”, Light Metals 1998, pp. 221 - 226.

2) T.B.Pedersen, The Søderberg Cell Technology – present performance, challenges and possibilities, Light Metals 2001, pp. 489 - 495

Recommended Reading

Alcorn, T.R., C.J. McMinn, and A.T. Tabereaux. Current efficiency in aluminium electrolysis by anode gas analysis (1988, pp. 683–695).

Asbjorsen, O.A., and J.A. Andersen. Kinetics and transport processes in the dissolution of aluminum oxide in cryolite melts (1977, Vol. 1, pp. 137–161).

Bagshaw, A.N., et al. Effect of operating conditions on the dissolution of primary and secondary (reacted) alumina powers in electrolytes (1985, pp. 649–659).

Brilloit, P., L.P. Lossius, and H.A. Øye. Melt penetration and chemical reactions in carbon cathodes during aluminium electrolysis I: Laboratory experiments (1993, pp. 321–330).

Chrenkova, M., et al. Density, electrical conductivity and viscosity of low melting baths for aluminium electrolysis (1996, pp. 227–232)

Dewing, E.W. Activities in Li_3AlF_6-Na_3AlF_6 melts (1985, pp. 737–749).

Dewing, E.W., and E.T. Van der Kouwe. Activities in the liquid system NaF-MgF_2-AlF_3 (1989, pp. 297–302).

Grjotheim, K., W.E. Haupin, and B.J. Welch. Current efficiency -- relating fundamental studies to practice (1985, pp. 679–694).

Grjotheim, K., et al. On the application of radiotracers in the aluminum industry (1971, pp. 133–164).

Haupin, W. Understanding boundary-layers (1997, pp. 319–323).

Haupin, W.E. Calculating thickness of containing walls frozen from melt (1971, pp. 188–194).

Haupin, W.E. Relaxation technique for calculating heat loss from an aluminum smelting cell (1963, pp. 139–152).

Hollingshead, E.A., and V.A. Braunwarth. Laboratory investigation of carbon anode consumption in the electrolytic production of aluminum (1963, pp. 31–50).

Johnson, A.R. Metal pad velocity measurements in aluminum reduction cells (1978, Vol. 1, pp. 45–58).

Kobbeltvedt, O., J. Thonstad, and S. Rolseth. On the mechanisms of alumina dissolution with relevance to point feeding aluminium cell (1996, pp. 421–427).

Kryukovsky, V.A., et al. Electrical conductivity of low melting cryolite melts (2006, pp. 409–413).

Kvande, H. Solubility of Al in NaF-AlF_3-Al_2O_3 melts (1980, pp. 171–182).

Liu, X., M.P. Taylor, and S.F. George. Crust formation and deterioration in industrial cells (1992, pp. 489–494).

Metson, J.B., et al. The anode effect revisited (2002, pp. 239–244).

Nissen, S.S., and D.R. Sadoway. Perfluorocarbon (PFC) generation in laboratory-scale aluminum reduction cells (1997, pp. 159–164).

Peacey, J.G., and G. W. Medlin. Cell sidewall studies at noranda aluminum (1979, pp. 475–492).

Richards, N.E. The dynamics of components of the anodic overvoltage in the alumina reduction cell (1998, pp. 521–529).

Richards, N.E., et al. Electrochemical analysis of alumina dissolved in cryolite melts (1995, pp. 391–404).

Røstum, A., A. Solheim, and A. Sterten. Phase diagram data in the system Na_3AlF_6 - Li_3AlF_3 - Al_2O_3 Part I: Liquidus temperatures for primary cryolite crystalization (1990, pp. 311–323).

Rye, K.A., M. Konigsson, and I. Solberg. Current redistribution among individual anode carbons in a Hall-Heroult prebake cell at low alumina concentrations (1998, pp. 241–246).

Shen, X.C., M. Hyland, and B. Welch. Top heat loss in Hall-Heroult cells (2008, pp. 501–504).

Solheim, A., and S. Åsmund. Activity of alumina in the system NaF - AlF_3 - Al_2O_3 at NaF/AlF_3 molar ratios ranging from 1.4 to 3 (1999, pp. 445–452).

Solheim, A., and S. Rolseth. Some surface and interfacial phenomena encountered in aluminium electrolysis (2001, pp. 469–474).

Solheim, A., and J. Thonstad. Heat transfer coefficients between bath and side ledge in aluminum cells: Model experiments (1983, pp. 425–435).

Sterten, A., and K. Hamberg. The NaF-AlF_3-Al_2O_3-Na_2O system: Activities of aluminum fluoride and sodium fluoride in melts saturated with alumina (1976, Vol.1, pp. 203–221).

Tabereaux, A.T. Phase and chemical relationships of electrolytes for aluminum reduction cells (1985, pp. 751–761).

Thonstad, J., P. Johansen, and E.W. Kristensen. Some properties of alumina sludge (1980, pp. 227–239).

Thonstad, J., and S. Rolseth. Equilibrium between bath and side ledge in aluminum cells: Basic principles (1983, pp. 415–424).

Thonstand, J., et al. On the anode effect in industrial aluminum cells (1984, pp. 825–839).

Tørklep, K., K. Kalgraf, and T. Nordbo. Alumina distribution in point-fed Hall-Heroult cells (1997, pp. 377–386).

Tørklep, K., and H.A. Øye. Viscosity of the melt system: NaF-AlF_3-Al_2O_3 (1979, pp. 373–384).

Utigard, T.A., et al. Visualization of the Hall-Heroult process (1994, pp. 233–240).

Yang, J-H., et al. Alumina solubility in KF-AlF_3 based low-temperature electrolyte system (2007, pp. 537–541).

Zhou, H-H., O. Herstad, and T. Østvold. Vapour pressure studies of and complex formation in NaF-AlF_3 and Na_3AlF_6 - MgF_2 melts (1992, pp. 511–520).

Zhu, H., and D.R. Sadoway. An electroanalytical study of electrode reactions on carbon anodes during electrolytic production of aluminum (2000, pp. 257–263).
Zhuxian, Q., F. Naixiang, and K. Grjotheim. On the electrochemical dissolution of aluminium in cryolite-alumina melts (1983, pp. 357–377).